Cancer Nano (2010) 1:35–46
DOI 10.1007/s12645-010-0005-1

ORIGINAL PAPER

Thermo-optical analysis and selection of the properties of absorbing nanoparticles for laser applications in cancer nanotechnology

Victor K. Pustovalov · L. G. Astafyeva · E. Galanzha · V. P. Zharov

Received: 9 April 2010 / Accepted: 8 August 2010 / Published online: 7 September 2010

Abstract Applications of nanoparticles (NPs) as photothermal (PT) and photoacoustic (PA) labels and agents for diagnosis and therapy of cancer and other diseases in laser medicine are fast growing areas of research. Many potential benefits include possibility for imaging with higher resolution and treatment of deeper tissues containing NPs, killing of individual abnormal cells, etc. Nevertheless, despite successful results, there is a lack of focused analysis of requirements to NPs for optimization of PT/PA applications, especially with pulsed lasers. Here, we present a platform for analysis of NP properties (e.g., optical, thermal, acoustic, structural, and geometric), allowing to select their parameters in the presence of different ambient tissues. The several types of NPs are described, which provide significant increased conversion of laser pulse energy in PT/PA phenomena. These NPs make it possible to use them with maximal efficiency for detection and killing single malignant cells labeled with minimal amount of NPs and in laser nanomedicine.

V. K. Pustovalov (✉)
Belarusian National Technical University,
pr. Independence 65,
220013 Minsk, Belarus
e-mail: pustovalovv@mail.ru

L. G. Astafyeva
Stepanov Institute of Physics,
National Academy of Sciences of Belarus,
pr. Independence 68,
220072 Minsk, Belarus

E. Galanzha · V. P. Zharov
Philips Classic Laser and Nanomedicine Laboratories,
University of Arkansas for Medical Sciences,
4301 W. Markham,
Little Rock, AR 72205, USA

Keywords Nanoparticle · Properties · Laser · Analysis · Optimization · Cancer

PACS 42.62.Be · 87.54.Br · 78.67.Bf

1 Introduction

Recent advances in photothermal (PT) and photoacoustic (PA) techniques based on nonradiative conversion of absorbed energy by nanoparticles (NPs) and following thermal and accompanied phenomena demonstrated its great potential. The PT/PA techniques may use NPs as exogenous contrast agents for therapy of cancer and infection or imaging tumor, blood vessels in deeper tissue in living organisms with higher resolution and sensitivity compared to other optical methods (Zharov et al. 2005a, b). Recently, various NPs demonstrated advantages as PT/PA agents for clinical use (Hirsch et al. 2003, 2006; Pitsillides et al. 2003; Zharov et al. 2003; Pissuwan et al. 2006; Huang et al. 2006; Jain et al. 2006; Blaber et al. 2009) because of their extremely high absorption for visible and near-infrared radiation with relatively deep penetration into most tissues, low toxicity, photostability, absence of photobleaching or blinking effects, and capacity for molecular targeting using appropriate bioconjugation with antibodies, proteins, and other ligands. Two gold NPs (GNPs) have already been approved for cancer-related clinical trials (Nanospectra Biosciences 2008). High absorption of radiation by NPs can be used for conversion of absorbed energy into NP thermal energy, heating of NPs itself and ambient tissue, and following PT/PA phenomena. These phenomena can be used in selective PT therapy when NPs are conjugated to antibodies (anti-EGFR) specifically targeted to malignant cells. This includes (but not limited) gold nanospheres

(Pitsillides et al. 2003; Zharov et al. 2003), nanoshells (Hirsch et al. 2003, 2006), nanorods (Huang et al. 2006; Eghtedari et al. 2007), and nanocages (Chen et al. 2007) among other NPs. Our experimental contribution includes first pioneer application of GNPs for detection and killing of individual tumor cells (Zharov et al. 2003), bacteria (Zharov et al. 2006), viruses (Everts et al. 2006), synergistic enhancement of PT/PA contrasts (Zharov et al. 2005a, b; Khlebtsov et al. 2006), the use ethanol (Kim et al. 2007), ultrasensitive PA/PT detection of single NPs, and cells labeled with NPs (Zharov et al. 2007).

However, despite long history of NP development and its application, it is still lack of systematic analysis of optimal parameters of NPs for using them as PT/PA agents in laser nanomedicine. Here, we propose a platform for analysis and optimization of properties of NPs as diagnostic tools and cell killers.

2 Phenomenological parameters and properties of laser–nanoparticle–tissue interactions

Optimization of different NP types is based on the investigation of the influence of different parameters of NP itself, laser pulses, and ambient tissues on efficiency of NP applications for laser diagnostics and therapy of cancer. The NPs have two basic geometries: spherical and cylindrical with various compositions including spherical homogeneous and core–shell two-layered NPs, gold nanorods.

Different parameters of laser radiation, NPs, and ambiences can influence on thermo-optical properties of absorbing NPs and determine the achievement of maximal efficacy of transformation of absorbed energy into PT/PA phenomena, including the increase of NP temperature T_0 and arising pressure p in ambient tissue. Among these parameters, we can note the next ones:

1. Laser radiation
   - (a) Pulse duration t_P
   - (b) Wavelength
   - (c) Energy density E_0 (intensity I_0)
2. Nanoparticle
   - (a) Material of NP with values of density, heat capacity, and optical properties
   - (b) Size
   - (c) Concentration of NPs in tissue
   - (d) Shape (spherical and cylindrical)
   - (e) Structure (homogeneous and core–shell)
3. Ambient tissue
   - (a) Coefficient of thermal conductivity, density, and heat capacity
   - (b) Coefficient of absorption, scattering, and extinction

When NPs are irradiated by short laser pulses with duration t_P, excitation and relaxation processes in the NPs lead eventually to conversion of absorbed laser energy into heat and subsequent PT and PA phenomena. To provide maximal efficiency of PT/PA process parameters of laser radiation, NP and ambient tissue should meet several requirements referred to as conditions and "confinements."

3 Influence of pulse duration on photothermal processes

3.1 Thermal confinement

To provide efficient heating of NPs without heat loss, in analogy to selective photothermolysis (Anderson and Parrish 1983), the pulse duration t_P should be less than the characteristic thermal relaxation time τ_T of NP cooling (Pustovalov et al. 2008):

$$t_P < \tau_T \qquad (1)$$

For nanosphere with radius r_0, $\tau_T \sim r_0^2 c_0 \rho_0 / 3k_\infty$, where c_0 and ρ_0 are the heat capacity and density of NP material, and k_∞ is the coefficient of thermal conductivity of ambient tissue. For gold nanosphere with r_0=30 nm in ambient water with $k_\infty = 6\times10^{-3}$ W/cmK, $\tau_T \sim 1.25$ ns. Under thermal confinement, the absorbed energy is almost instantaneously (characteristic time, $\sim 10^{-12}$ s) transformed in thermal energy leading to immediate increase NP temperature. The fulfillment of thermal confinement means achievement of maximal value of NP temperature $T_{max} = T_0(t_P)$ practically without heat exchange with ambience for $t_P < \tau_T$. Case $t_P > \tau_T$ can be used for heat exchange of NPs with ambient tissue and its heating.

3.2 Acoustic (stress) confinement

The most efficient transformation of thermal energy into acoustic energy occurs under the condition:

$$t_P < \tau_A \qquad (2)$$

where $\tau_A = 2r_0/c_s$ is the transit time of the acoustic wave traveling through distance of $2r_0$, and c_s is the speed of sound in tissue. For nanosphere with r_0=30 nm in water with $c_s = 1.5\times10^5$ cm/s, $\tau_A \sim 40$ ps. The PA response under Eq. 2 includes component associated with thermal expansion of NPs into ambient soft tissue (biofluid). We have to note that $\tau_A << \tau_T$, and it is not possible to create PA response from fluid around NPs heated by heat diffusion from NPs during long laser pulse action (at $t_P > \tau_T$) when Eq. 1 is not valid.

We estimate the fulfillment of thermal and acoustic confinements (Eqs. 1 and 2) for some values of pulse duration t_P and characteristic radii $r_0 \sim 10$–40 nm of spherical NPs:

$t_P < \tau_A$, τ_T — Pulse duration meets both thermal (Eq. 1) and acoustic (Eq. 2) confinements for pico- ~1–10 ps and femtosecond ~100 fs pulse duration range

$\tau_A < t_P < \tau_T$ — Pulse duration meets thermal confinement (Eq. 1), but does not meet acoustic confinement (Eq. 2) for subnanosecond range of pulse duration, $t_P \sim 0.1$ ns

$t_P > \tau_A$, τ_T — Pulse duration does not meet both acoustic and thermal confinements (Eqs. 1 and 2) for nanosecond range of pulse duration, 1–10 ns and more

4 Analysis of the parameters of homogeneous spherical gold nanoparticles placed in different ambiences and optimization by selection of their thermo-optical properties

4.1 Optical properties

We investigate optical properties and conditions of optical confinement of NPs in tissues. In most medical applications, NPs are surrounded by bioliquids such as blood, lymph, or protein. We will investigate the influence of different liquid ambiences on parameters of spherical homogeneous GNPs.

4.1.1 Optical NPs confinement

The absorption of laser radiation by NPs should be greater than absorption of radiation by ambient tissue to enhance contrast of NPs and should be greater than scattering of radiation by NPs because of harmful action of scattered radiation on tissue. Extinction of laser radiation by NPs should be smaller than extinction of radiation by ambient tissue for effective use of NPs for PT therapy in deeper tissue. This difference between coefficients of absorption $\acute{\alpha}_{abs}$, scattering $\acute{\alpha}_{sca}$, and extinction $\acute{\alpha}_{ext}$ of laser radiation by NPs and the coefficients of absorption β_{abs} and extinction β_{ext} of laser radiation by ambient tissue should provide optical confinement:

$$\begin{aligned} &\acute{\alpha}_{abs} = \pi N_0 r_0^2 K_{abs} > \beta_{abs}, \\ &\acute{\alpha}_{abs} > \acute{\alpha}_{sca} = \pi N_0 {r_0}^2 K_{sca} (K_{abs} > K_{sca}), \\ &\acute{\alpha}_{ext} = \pi N_0 r_0^2 K_{ext} < \beta_{ext} \end{aligned} \tag{3}$$

where N_0 is the concentration of NPs in tissue; r_0 is the radius of spherical NP or equivolume sphere for nanorod; K_{abs}, K_{sca}, and K_{ext} are the efficiency factors of absorption, scattering, and extinction of laser radiation, respectively, by NP (Bohren and Huffman 1983; Pustovalov and Babenko 2004). Analysis of optical properties of NPs and tissues, concentration, and sizes of NPs can give us appropriate types of NPs.

4.1.2 Gold nanoparticle in water

Water is the main component of soft tissues, blood, etc., and so this one was chosen for calculation. Figures 1 and 2 present efficiency factors of absorption K_{abs}, scattering K_{sca}, and extinction K_{ext} of laser radiation with wavelengths $\lambda = 532$ and 800 nm by spherical GNPs in the range of radii 5–100 nm in water (lines 1) calculated on

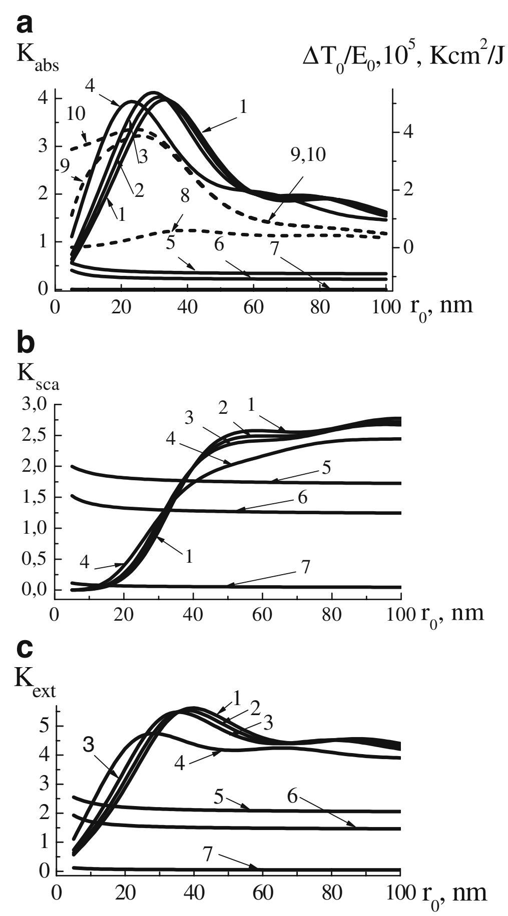

Fig. 1 Efficiency factors of absorption K_{abs} (**a**), scattering K_{sca} (**b**), and extinction K_{ext} (**c**) of laser radiation with wavelength 532 nm by gold NPs with the following shapes and ambiences: sphere placed in water (*1*), in blood (*2*), in protein (*3*), in ethanol (*4*), and infinite rod (*5–7*) in water with angles between direction of laser radiation propagation and main axis of nanorod: 90° (*5*), 45° (*6*), and 0° (*7*). Parameters $\Delta T_0/E_0$ for spherical gold particles in water for $t_P = 1 \times 10^{-8}$ (*8*), 1×10^{-10} (*9*), 1×10^{-12} (*10*) *c*, $\lambda = 532$ nm. *Solid lines* (*1–7*) refer to the left axis, and *short dashed lines* (*8–10*) refer to the right axis. Sphere radii are in the range $r_0 \sim 5$–100 nm, for rod r_0 means its radius

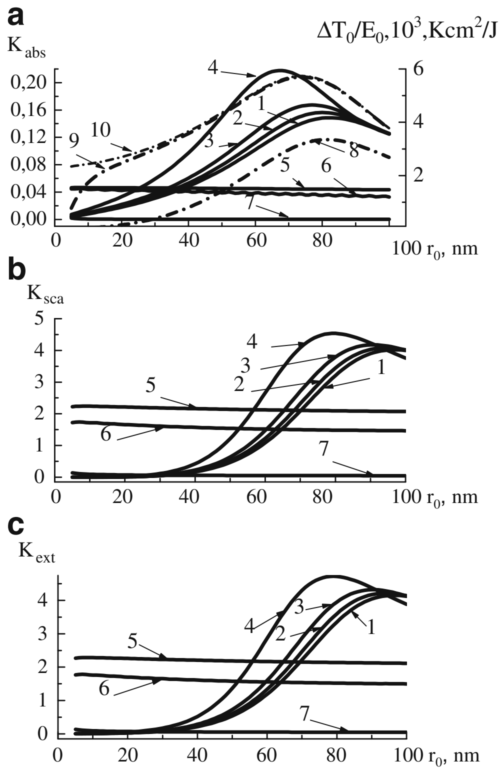

Fig. 2 Factors K_{abs} (**a**), K_{sca} (**b**), and K_{ext} (**c**) for laser radiation with wavelength 800 nm and gold NPs with the following shapes and ambiences: sphere placed in water (*1*), in blood (*2*), in protein (*3*), in ethanol (*4*), and infinite rod (*5–7*) in water with angles between direction of laser radiation propagation and main axis of nanorod: 90° (*5*), 45° (*6*), and 0° (*7*). Parameters $\Delta T_0/E_0$ for spherical gold particles in water for $t_P=1\times10^{-8}$ (*8*), 1×10^{-10} (*9*), 1×10^{-12} (*10*) *c*, $\lambda=$ 800 nm. *Solid lines* (*1–7*) refer to the left axis, and *short dash-dot lines* (*8–10*) refer to the right axis. Sphere radii are in the range $r_0\sim5$–100 nm, for rod r_0 means its radius

the base of Mie theory (Bohren and Huffman 1983). Optical parameters for gold and water (indexes of refraction and absorption) were taken from Johnson and Christy (1972) and Zuev (1970).

For wavelength $\lambda=532$ nm, K_{abs} for gold spheres in the range $5<r_0<50$ nm has maximal values $K_{abs}\sim3.9$–3.6 for $r_0\sim25$–40 nm. Factor K_{sca} for radiation 532 nm lies in the limits $K_{sca}\sim0.1$–2.5 and $K_{abs}>K_{sca}$ for the range $5<r_0<50$ nm. Values of $K_{abs}<K_{sca}$ for the range $50<r_0<100$ nm. Taking into account the correlation between the values of K_{abs}, K_{sca}, and K_{ext} and the possibility to select the values of NP concentration N_0, we can achieve the fulfillment of optical confinement (Eq. 3) for the range $5<r_0<50$ nm.

For $\lambda=800$ nm, K_{abs} has lower values in the limit $\sim1\times10^{-2}$–2×10^{-1} and $K_{sca}\sim1\times10^{-2}$–4 for the range $r_0\sim5$–100 nm and $K_{sca}\geq K_{abs}$. GNPs are bad absorbers for wavelength 800 nm and cannot be used for our purposes.

4.1.3 Gold nanoparticle in blood, protein, and ethanol

GNPs can be placed in blood ambience and used for thermal action in blood vessels, hemorrhages, etc. Normal human whole blood consists of about 55 vol.% plasma (90% water and 10% proteins) and 45 vol.% cells (erythrocytes, leucocytes, and thrombocytes). Figures 1 and 2 present efficiency factors of K_{abs}, K_{sca}, and K_{ext} for spherical GNPs in the range of radii 5–100 nm placed in blood for laser wavelengths $\lambda=532$ and 800 nm (lines 2). Optical (Ivanov et al. 1988) and thermophysical (Welch and van Gemert 1995) properties of blood are close to water ones, and factors K_{abs}, K_{sca}, and K_{ext} for GNPs in blood are close to analogous values for water ambience (compare lines 1 and 2 in Figs. 1 and 2). Results of laser action on GNPs in blood will be close to results of analogous action on GNPs in water.

Figures 1 and 2 present factors of K_{abs}, K_{sca}, and K_{ext} for laser wavelengths $\lambda=532$ and 800 nm and for spherical GNPs in the range of radii 5–100 nm placed in protein (lines 3). Optical and thermophysical properties of protein (egg white; Arakawa et al. 2001; Opielinski 2007) are close to properties of water (Zuev 1970) because normal hen's white egg consists of about 80–90% water. For wavelength 532 nm, maximal values of K_{abs} lie in the range $r_0\sim20$–40 nm, and they are approximately equal to maximal values of K_{abs} for water ambience. Consequently, the heating and maximal temperature of GNPs under laser action with $\lambda=$ 532 nm in protein will be approximately equal to values for NP in water. For wavelength $\lambda=800$ nm, values of K_{abs} and K_{sca} are greater than analogous parameters for water and blood ambiences. Heating of GNPs and scattering of radiation in protein will be higher in comparison with mentioned ambiences for $\lambda=800$ nm.

Possible variant of substitution of ambient water for GNPs could be ethanol. Figures 1 and 2 present efficiency factors of K_{abs}, K_{sca}, and K_{ext} for spherical GNPs in the range of radii 5–100 nm placed in ethanol for laser wavelengths $\lambda=532$ and 800 nm (lines 4). Optical parameters of ethanol were taken from Rheims et al. (1997). Maximal values of K_{abs} lie in the range $K_{abs}\sim3.5$–3.7 for $\lambda=532$ nm and $r_0\sim20$–35 nm. Values of K_{sca} are lower for $40<r_0<100$ nm in comparison with the ones for GNP in water for $\lambda=532$ nm. Maximal values of K_{abs}, K_{sca}, and K_{ext} for $\lambda=800$ nm are greater than the ones for GNPs in other ambiences.

4.2 Thermal and acoustic properties

4.2.1 Thermal properties

We investigate the thermal and acoustic properties of spherical homogeneous NPs in liquid ambience. Characteristic time τ_T is equal to $\tau_T \sim 3.2\times10^{-11}$–$3.2\times10^{-9}$ s for the range r_0=5–50 nm and for water $k_\infty=6\times10^{-3}$ W/cmK, $\tau_T\sim$ 1.25 ns for r_0=30 nm. The fulfillment of thermal confinement $t_P<\tau_T$ (Eq. 1) for most interesting range of r_0, $25<r_0<40$ nm, means that the value of t_P will be in the range of pulse durations, $t_P<1\times10^{-9}$ s. Parameter $\Delta T_0/E_0$ can be used for determination of thermo-optical properties of NPs, and it is equal (Pustovalov et al. 2008):

$$\frac{\Delta T_0}{E_0} = \frac{K_{abs} r_0}{4k_\infty t_P}\left[1-\exp\left(-\frac{3k_\infty t_P}{c_0\rho_0 {r_0}^2}\right)\right] \tag{4}$$

where $\Delta T_0=T_{max}-T_\infty$, T_∞ is the initial temperature, $T_{max}=T_0(t_P)$. Equation 4 may be viewed as NP heating efficacy depending on r_0, K_{abs} (λ), ρ_0, c_0, t_P, and k_∞ under action of radiation energy density E_0. This parameter determines the increase of NP temperature under action of laser radiation with energy density value equal to 1 J/cm^2. Heating efficacy parameter $\Delta T_0/E_0$ under conditions $t_P<\tau_T$ and $t_P>\tau_T$ will be approximately determined by (see Eq. 4)

$$t_P > \tau_T\, \frac{\Delta T_0}{E_0} \approx \frac{K_{abs} r_0}{4k_\infty t_P} \tag{5}$$

$E_0=I_0t_P$ is the laser energy density. This parameter determines the heating of NP and depends on t_P and combination K_{abs}/r_0 under fixed values c_0 and ρ_0 for gold. The selection of mentioned parameters in Eqs. 4 and 5 can provide maximal values of ΔT_0 for concrete E_0.

Figures 1 and 2 present dependencies of parameter $\Delta T_0/E_0$ (Eq. 4) for pulse duration $t_P=1\times10^{-8}$, 1×10^{-10}, and 1×10^{-12} s for laser wavelength λ=532 (Fig. 1) and 800 nm (Fig. 2) on radius r_0 of spherical GNPs. The condition of "short" pulses $t_p<\tau_T$ is applicable for $t_P=1\times10^{-12}$ s for all range of r_0, $5<r_0<100$ nm, and for $t_P=1\times10^{-10}$ s in the range $r_0>30$ nm. The values of $\Delta T_0/E_0$ (lines 9 and 10 in Fig. 1) for $r_0>30$ nm coincide to each other for $t_P=1\times10^{-10}$ and 1×10^{-12} s because for the case of "short" pulses parameter, $\Delta T_0/E_0$ does not depend on t_P (see Eq. 5). Only for $r_0<30$ nm, these curves are different ones. Under condition of "short" pulses $t_P<\tau_T$ parameter, $\Delta T_0/E_0$ depends on combination K_{abs}/r_0, accordingly Eq. 5, describing the increasing and decreasing of the value of $\Delta T_0/E_0$. Maximal value of $\Delta T_0/E_0\sim4\times10^5$ for $r_0\sim30$ nm and for $t_P<1\times10^{-9}$ s under laser energy density E_0=0.005 J/cm^2, heating of such NP could achieve 2×10^3 K.

For "long" pulses, $t_P=1\times10^{-8}$ s$>\tau_T$, for all range of r_0= 5–100 nm, and value of $\Delta T_0/E_0$ is much smaller than value of this one for the case of short pulses because of dependence $\Delta T_0/E_0\sim1/t_P$ (see Eq. 5). Behavior of $\Delta T_0/E_0$ (see Figs. 1 and 2) depends on combination of K_{abs} r_0 accordingly (Eq. 5).

For λ=800 nm, the values of $\Delta T_0/E_0$ are much smaller than the ones for λ=532 nm because of low values of K_{abs}, and combination of K_{abs} r_0 describes the behavior of $\Delta T_0/E_0$.

4.2.2 Acoustic properties

PA signal excited in a medium around NP under action of short laser pulse consists of pressure wave. The most important case for effective destruction of ambient tissue around NP is determined by the following conditions. (1) The thickness of the heated layer of the ambient tissue is small compared to NP radius r_0: $r_0 > \sqrt{\chi t_P}$. (2) All volume of NP was heated during laser pulse action: $r_0 < \sqrt{\chi_0 t_P}$, χ, and χ_0 are coefficients of thermal diffusivity of ambient tissue and NP material, respectively. The pressure amplitude p of the spherical acoustic wave excited is determined by the thermal expansion of NP (Karabutov et al. 1996):

$$p(t) = \frac{I_0 K_{abs} {r_0}^2 \rho \beta_0}{4r\rho_0 c_0}\frac{\partial f}{\partial t} \tag{6}$$

ρ is the density of ambient tissue, β_0 is the effective thermal expansion coefficient of the NP material, r is the radius of observation point, and $f(t)$ function defines the time dependence of the laser radiation intensity. Maximal efficacy of transformation of heat energy into acoustic pressure will be determined by parameter p/I_0 or p/E_0 (see Eq. 6):

$$\frac{p(t)}{E_0} = \frac{K_{abs} {r_0}^2 \rho \beta_0}{4r\rho_0 c_0 t_P}\frac{\partial f}{\partial t}. \tag{7}$$

4.2.3 Analysis of thermal and acoustic NP properties in water and ethanol

Compare some thermophysical parameters of water and ethanol. Heating of fixed volume of liquid to some value of temperature will be determined by parameter ρc (see Eq. 8), and for ethanol and water, it is equal to 1.92 and 4.18 J/cm^{3}K (Kreith and Black 1980; Grigor'ev and Meilikhov 1991). We need to spend energy for heating of fixed volume (mass) of water up to 2.2 times greater in comparison with ethanol. Heat conduction and diffusivity coefficients for ethanol are smaller up to 3.5 and 1.5 times than these ones for water (Kreith and Black 1980; Grigor'ev and Meilikhov 1991), and as a result, the thickness of heated layer around NP in ethanol will be smaller than in water. Substitution of water by ethanol leads to increasing of value τ_T up to 3.5 times and easier fulfillment of thermal confinement (Eq. 1). Coefficient of thermal volume expansion for ethanol β_0 is up to five times greater compared to water (1.1×10^{-3} 1/K vs. 2.1×10^{-4} 1/K;

Kreith and Black 1980; Grigor'ev and Meilikhov 1991) that can lead to formation of stronger pressure wave in ambient tissue (see Eq. 3) and facilitation of acoustic confinement. As a result of all comparisons, the level of laser energy required to produce the PT and PA effects around GNP in ethanol is dramatically decreased up to one-order magnitude in comparison with water.

It was experimentally found that replacement of water with ethanol led to an increase in both PT and PA signals from NPs of about five- to sevenfold at the same level of laser energy (Kim et al. 2007). This approach can also be applied for PT laser cancer therapy with GNP because particular percutaneous ethanol injection is already used for disinfection purposes and to treat liver tumor.

Characteristic time τ_A for r_0=25–40 nm, and water with $c_s=1.5\times10^5$ cm/s is equal to $\tau_A\sim3.3–5.5\times10^{-11}$ s. The fulfillment of acoustic confinement $t_P<\tau_A$ (Eq. 2) for the range of r_0, $25<r_0<40$ nm, means in this case, $t_P<3\times10^{-11}$ s; value of t_P is thus in the picosecond ranges. Parameter p/I_0 (see Eq. 3) determines the dependence of efficacy of transformation of heat energy into acoustic energy on parameters of NP: r_0, ρ_0, c_0, β_0, K_{abs}, and density of ambient liquid ρ. We estimate the value of p for GNP, r_0=40 nm, t_P=200 ps, parameters of ambient tissue are equal parameters of water, K_{abs} is from Fig. 1 for wavelength 532 nm, thermophysical parameters are from Kreith and Black (1980), $I_0=I_{max}t$ for time interval 0, $t_P/2$ with $I_{max}=1\times10^{18}$ W/scm^2 and $I_0=1\times10^8$ W/cm^2 at $t=t_P/2$, and as a result, $p\sim25$ atm. We see real possibility to use PA mode for our purposes.

Spherical GNPs with sizes in the range $25<r_0<40$ nm for wavelength 532 nm can be used for laser thermal regimes for values of pulse durations $t_P<1\times10^{-9}$ s and for acoustic regime for $t_P<3\times10^{-11}$ s.

Spherical homogeneous GNPs with sizes in the range $20<r_0<40$ nm can be used for laser thermal and acoustical regimes for λ=532 nm under fulfillment of all confinement conditions with approximate accuracy in water, protein, and blood ambiences. The use of GNPs in ethanol ambience leads to increase of efficacy. The use of infrared wavelengths (λ=800 nm) and spherical homogeneous GNPs leads to significant decrease of efficacy.

5 Analysis and optimization of the properties of spherical two-layered core–shell nanoparticles by selection of their parameters

Spherical core–shell NPs have great potential for diagnostics and therapeutic applications due to strongly enhanced surface plasmon resonance for scattering and absorption and tuning of absorption band in visible and near-infrared region (Hirsch et al. 2003, 2006) by varying the relative core size and shell thickness. They include various compositions including solid absorbing core with nonabsorbing shell, dielectric core with absorbing coating (silica core and gold shells), etc. The results of analysis and optimization of two-layered core–shell NPs placed in water are presented on the base of selection of optical, structural, and thermophysical properties for some types of NPs. Optical properties of two-layered core–shell NPs were calculated on the base of extended Mie theory (Pustovalov et al. 2009).

5.1 Heating of spherical two-layered core–shell nanoparticles by short laser pulses

A two-layered particle consists of a spherical homogeneous core of radius r_0 enveloped by the spherically symmetric homogeneous shell of radius r_1. We should take into account that lines in Figs. 3, 4, and 5 are presented for the values of radius $r_0+\Delta r_0$ with thickness of shell $\Delta r_0=r_1-r_0$. Process of laser heating of two-layered core–shell NP

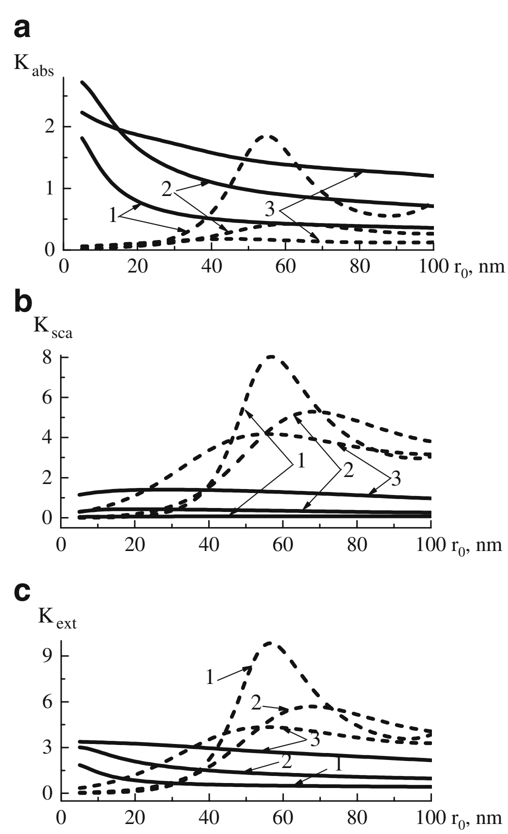

Fig. 3 Factors K_{abs} (**a**), K_{sca} (**b**), and K_{ext} (**c**) for laser radiation with wavelengths 532 (*solid line*) and 800 nm (*short dashed line*) and water core–gold shell spherical nanoparticles for the range of radii r_0=5–100 nm and thicknesses of shell Δr_0=10 (*1*), 20 (*2*), and 40 (*3*) in water

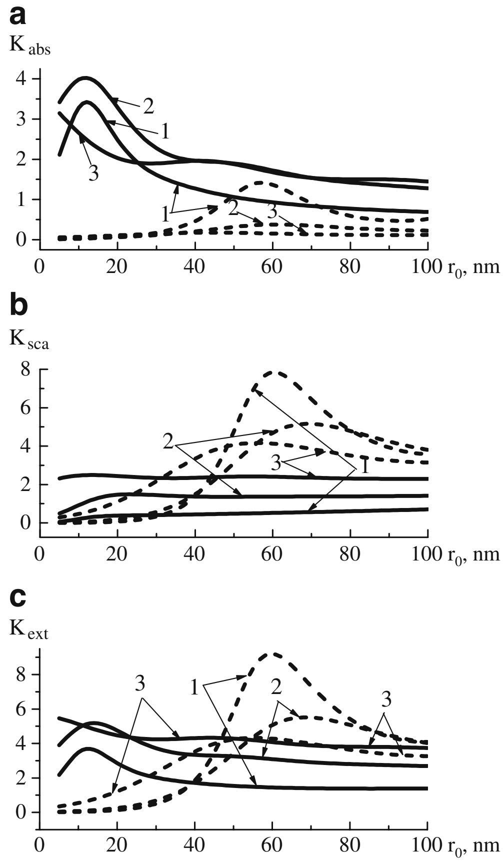

Fig. 4 Factors K_{abs} (**a**), K_{sca} (**b**), and K_{ext} (**c**) for laser radiation with wavelengths 532 (*solid line*) and 800 nm (*short dashed line*) and air core–gold shell spherical nanoparticles for r_0=5–100 nm and Δr_0=10 (*1*), 20 (*2*), and 40 (*3*) in water

and its cooling after the end of laser pulse action is described by Eq. 8:

$$(\rho_0 c_0 V_0 + \rho_1 c_1 V_1)\frac{dT_{10}}{dt} = I_0(t)K_{abs}S_{10} - J_C S_1, \tag{8}$$

with the initial condition:

$$T_{10}(t=0) = T_\infty \tag{9}$$

T_{10} is uniform temperature over the particle volume, ρ_0, c_0, and ρ_1, c_1 are the heat capacity and density of core and shell materials accordingly; J_C is the energy flux density removed from the particle surface by heat conduction. Volumes V_0 and V_1 of core and shell are respectively equal: $V_0 = \frac{4}{3}\pi r_0^3$, $V_1 = \frac{4}{3}\pi\left(r_1^3 - r_0^3\right)$; $S_{10} = \pi r_1^2$ is the square of NP cross-section, and S_1=$4\pi r_1^2$ is the surface area of a spherical particle of radius r_1.

Maximal value of spherical NP temperature T_{max} at the end of laser pulse action with pulse duration t_P under constant radiation intensity I_0=const during t_P, we find from Eq. 8, taking into account the methodology of Pustovalov (2005):

$$T_{max} = T_\infty + \frac{I_0 K_{abs} r_1}{4k_\infty} \times \left[1 - \exp\left(-\frac{3k_\infty t_P}{c_0\rho_0 r_0{}^2 \frac{r_0}{r_1}\left(1 + \frac{c_1\rho_1}{c_0\rho_0}\left(\frac{r_1{}^3}{r_0{}^3} - 1\right)\right)}\right)\right] \tag{10}$$

Characteristic thermal time for cooling of core–shell NP from Eq. 10 is equal:

$$\tau_{T1} = \frac{c_0\rho_0 r_0^2}{3k_\infty}\frac{r_0}{r_1}\left(1 + \frac{c_1\rho_1}{c_0\rho_0}\left(\frac{r_1^3}{r_0^3} - 1\right)\right) = \tau_T\frac{r_0}{r_1}\left(1 + \frac{c_1\rho_1}{c_0\rho_0}\left(\frac{r_1^3}{r_0^3} - 1\right)\right) \tag{11}$$

and it is determined by core ρ_0, c_0, r_0 and shell ρ_1, c_1, r_1 parameters, where $\tau_T = \frac{c_0\rho_0 r_0^2}{3k_\infty}$.

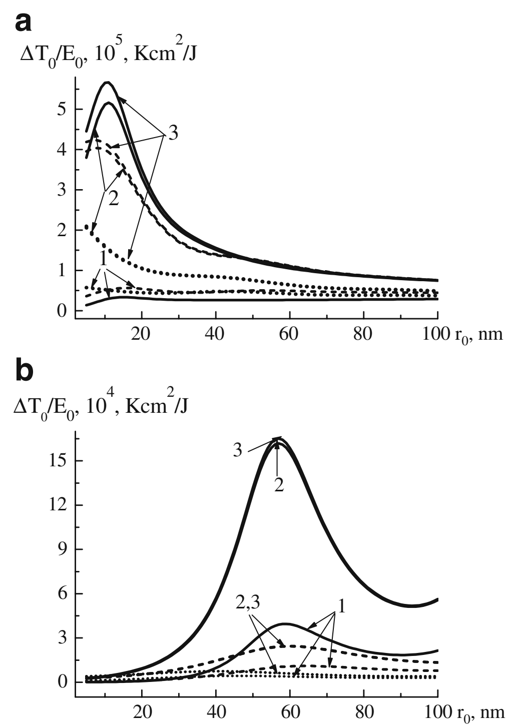

Fig. 5 Parameters $\Delta T_0/E_0$ for spherical two-layered air–gold particles in water for t_P=1×10^{-8} (*1*), 1×10^{-10} (*2*), and 1×10^{-12} s (*3*) for λ=532 (**a**) and 800 nm (**b**) for the range of radii r_0=5–100 nm and thicknesses of shell Δr_0=10 (*solid line*), 20 (*short dashed line*), and 40 nm (*dotted line*)

For core–shell NPs heating efficacy parameter, $\Delta T_0/E_0 = (T_{max} - T_\infty)/E_0$ is determined by

$$\frac{\Delta T_0}{E_0} = \frac{K_{abs} r_1}{4k_\infty t_P} \times \left[1 - \exp\left(-\frac{3k_\infty t_P}{c_0\rho_0 r_0^2 \frac{r_0}{r_1}\left(1 + \frac{c_1\rho_1}{c_0\rho_0}\left(\frac{r_1^3}{r_0^3} - 1\right)\right)}\right)\right] \tag{12}$$

For "short" laser pulses with pulse duration $t_P < \tau_{T1}$, the loss of heat from the NP by heat conduction during the time t_P can be ignored. For "long" laser pulses $t_P > \tau_{T1}$, the loss of heat from the particle by heat conduction will be significant. For "short" and "long" pulses from Eq. 12, we can get

$$t_P < \tau_{T1} : \frac{\Delta T_0}{E_0} \approx \frac{3K_{abs} r_1^2}{4\rho_0 c_0 r_0^3\left[1 + \frac{c_1\rho_1}{c_0\rho_0}\left(\frac{r_1^3}{r_0^3} - 1\right)\right]}, \qquad t_P > \tau_{T1} : \frac{\Delta T_0}{E_0} \approx \frac{K_{abs} r_1}{4k_\infty t_P} \tag{13}$$

These parameters (Eqs. 12 and 13) are determined by core and shell geometrical, optical, and material characteristics. Mutual feature for core–shell NPS is the approximation of their properties to the properties of homogeneous NPs from shell material when mass of shell will be greater than the mass of core.

5.2 Core–shell liquid–gold nanoparticles

Core–shell liquid (water)–gold NPs can be used for laser release of different liquid drugs on the target when drug can be placed inside NP in its core. Figure 3 presents factors of K_{abs}, K_{sca}, and K_{ext} of laser radiation with wavelengths 532 and 800 nm by water–gold spherical NPs in the range of core radii r_0=5–100 nm and thicknesses of shell Δr_0=10, 20, and 40 nm. Calculation of the absorption, scattering, and extinction factors of two-layered spherical NPs was made on the base of extended Mie theory (Kattawar and Hood 1976; Bhandari 1985). Maximal values of K_{abs}~2.7 for λ=532 nm lie close to r_0~5 nm and Δr_0=20 nm, and for λ=800 nm, value K_{abs}~1.8 lies in the range r_0~50–60 nm and Δr_0=10 nm. The increase of shell thickness Δr_0 increases the values of K_{abs}, K_{sca}, and K_{ext} for λ=532 nm. In the range of NP sizes, r_0~5–100 nm, Δr_0=10–40 nm $K_{abs} > K_{sca}$ for 532 nm, and the conditions of optical confinement can be fulfilled by variation of concentration N_0. In this case, NPs could be viewed as strong absorbers and weak scatterers. For wavelength 800 nm in the range r_0~10–100 nm, Δr_0=10–40 nm $K_{abs} < K_{sca}$, and condition of optical confinement (Eq. 3) is not fulfilled.

Optical properties of nanoshells with silica core and gold shell were investigated (Hirsch et al. 2003, 2006). Efficiency factors of water–gold and silica–GNPs show analogous dependencies of factors K_{abs}, K_{sca}, and K_{ext} on r_0 because optical parameters of silica for wavelengths 532 and 800 nm (Grigor'ev and Meilikhov 1991; Palik 1985) are close to optical parameters of water (Zuev 1970). Main advantage of silica–gold and water–GNPs is the possibility to tune their optical properties in visible and near-infrared regions between 500 and 1,000 nm. Under NP overheating because of absorption of laser energy, vapor bubble can be formed inside NP core (Pustovalov et al. 2008) with subsequent explosion of NP and release of drug on target.

Characteristic thermal relaxation time τ_{T1} will be defined by Eq. 11, taking into account thermophysical parameters both core and shell, for example, for r_0=30 nm and Δr_0=10, 20 nm τ_{T1} is equal accordingly τ_{T1}=2.1; 3.5 ns. The condition of acoustic confinement $t_P < 2r_1/c_s$ is the same one as for homogeneous NP with radius r_1. Parameter $c_0\rho_0$ for water is bigger than for gold, and it needs to spend additional energy to heat such NP in comparison with pure GNP.

5.3 Core–shell air–gold nanoparticles

Figure 4 presents factors of K_{abs}, K_{sca}, and K_{ext} of laser radiation with wavelengths 532 and 800 nm by air core gold shell spherical NPs in the range of radii r_0=5–100 nm and thicknesses of shell Δr_0=10, 20, and 40. Optical properties of air were taken from Grigor'ev and Meilikhov (1991). Maximal value of K_{abs} is equal to K_{abs}~4.0 for λ=532 nm and r_0~10–20 nm, Δr_0=20 nm. Values of K_{abs} are approximately equal to values for homogeneous GNPs, but values of K_{sca} are bigger than for pure GNPs for r_0~5–40 nm. For λ=800 nm K_{abs}~1.5 in the range r_0~50–60 nm, Δr_0=10 nm. The increase of shell thickness Δr_0>20 nm decreases the values of K_{abs} and approximates their properties to properties for homogeneous GNPs. In the range of NP sizes r_0~5–60 nm, Δr_0=10 and 20 nm $K_{abs} > K_{sca}$ for 532 nm and by variation of concentration of N_0 conditions of optical confinement (Eq. 3) can be fulfilled.

Figure 5 presents parameters $\Delta T_0/E_0$ for spherical two-layered air–gold particles in water for $t_P = 1\times10^{-8}$, 1×10^{-10}, and 1×10^{-12} s, λ=532 and 800 nm for the range of radii r_0=5–100 nm and thicknesses of shell Δr_0=10, 20, and 40 nm. The condition of "short" pulses $t_P < \tau_{T1}$ is applicable for $t_P = 1\times10^{-10}$ and 1×10^{-12} s for the ranges of radii r_0> 20 nm and thicknesses of shell Δr_0=10 and 20 nm. Increasing of t_P leads to decreasing the value of $\Delta T_0/E_0$ accordingly, Eq. 13, for $t_P > \tau_{T1}$.

Energy spent for air (gas)–gold NP heating can be decreased up to a few times in comparison with pure GNP with equal outer radius, because of lower value of $c_0\rho_0$ for air core, for example, up two times for $\Delta r_0 \sim 0.2\ r_1$. The feature of the practical use of air (gas)–GNPs is the possibility of the NP destruction because of increase of gas pressure with increase of NP temperature under absorption of laser energy and pressure can be higher than the durability limit of shell. This mode could be used for fragmentation of NPs and nanophotothermolysis of cancer cells (Pustovalov et al. 2008; Letfullin et al. 2006) under much lower value of laser intensity I_0 in comparison with fragmentation of homogeneous GNP because of optical breakdown or other nonlinear mechanisms.

5.4 Gold core–protein shell nanoparticles

For molecular targeting, external NP surface is functionalized with shell from different ligands including DNA, antibodies, proteins, etc. Figure 6 presents factors of K_{abs}, K_{sca}, and K_{ext} of laser radiation with wavelengths 532 and 800 nm by gold core–protein shell spherical NPs placed in water in the range of radii r_0=5–100 nm and Δr_0=2, 5, 10, and 20 nm. Optical properties of protein were taken from Opielinski (2007). Maximal value $K_{abs} \sim 3.7$ for λ=532 nm

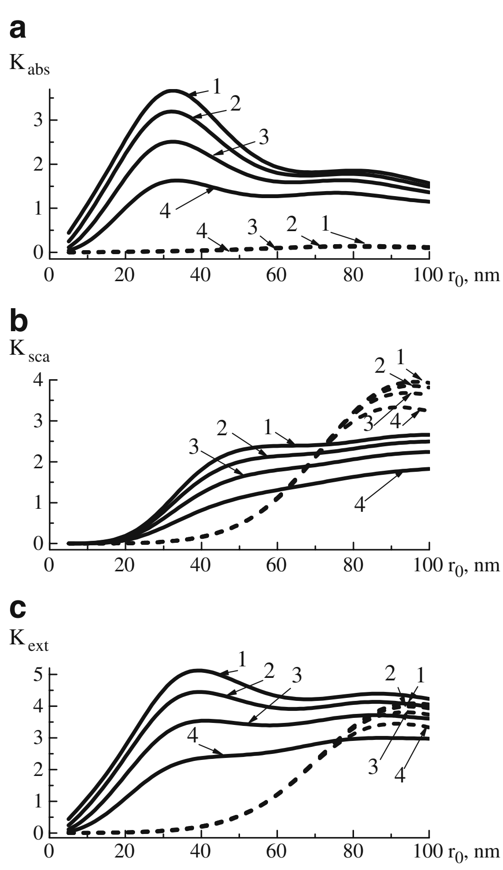

Fig. 6 Factors K_{abs} (**a**), K_{sca} (**b**), and K_{ext} (**c**) for laser radiation with wavelengths 532 (*solid line*) and 800 nm (*short dashed line*) and gold core–protein shell spherical nanoparticles for r_0=5–100 nm and Δr_0= 2 (*1*), 5 (*2*), 10 (*3*), and 20 (*4*) in water

for $r_0 \sim 30$–35 nm and Δr_0=2 nm. Factors K_{abs} and K_{sca} are decreasing with increasing of Δr_0 up to 20 nm. Maximal value K_{abs} is equal to $K_{abs} \sim 10^{-1}$–10^{-2}, and K_{sca} increases up to ~3–4 in the range $r_0 \sim 80$–100 nm, and these NPs are bad absorbers and scatterers in the range $r_0 \sim 5$–50 nm for λ=800 nm. Nonabsorbing layer of protein with different index of refraction in comparison with ambient bioliquid can lead to decreasing of absorption efficiency factor of GNP.

5.5 Gold core–polymer shell nanoparticles

To reduce toxicity and prolong circulation time, NPs are coated with thin polymer layer (e.g., PEG or Dextran). Thermal confinement of two-layered NPs could be improved by using a material of external layer with low thermal conductivity like some polymer materials. The heat flux density J_C from NP will be determined by the equation: $J_C = -\left(k_1 \frac{\partial T}{\partial r}\right)\Big|_{r_0}$. Decreasing the value of k_1 means decreasing J_C and conservation energy inside NP. Typical values of k_1 for polymer are approximately equal for photoroplast $k_1 \sim 2.3 \times 10^{-3}$ W/cmK, polystirol $k_1 \sim 1.6 \times 10^{-3}$ W/cmK (Grigor'ev and Meilikhov 1991), and much smaller in comparison with value $k_1 = 6 \times 10^{-3}$ W/cmK for water. Decreasing the value of k_1 leads to increasing the values of τ_T, τ_{T1}, and increasing the range of time for $t_P < \tau_T$, τ_{T1} (Grigor'ev and Meilikhov 1991). Decreasing the thermal diffusivity χ of ambient medium will lead to decreasing of thickness of heated layer during laser pulse action $\Delta r \sim (\chi t_P)^{1/2}$. The advantage of the use of such two-layered NP could be the promotion of the fulfillment of thermal and acoustic confinements with increasing of t_P.

6 Influence of nanoparticle shape on its properties

6.1 Gold nanorods in water

Figures 2 and 3 present factors K_{abs}, K_{sca}, and K_{ext} for laser radiation with wavelength λ=532 (Fig. 2) and λ=800 nm (Fig. 3) for infinite gold nanorods (GNRs) with angles between the direction of laser radiation propagation and main axis of nanorod: 0°, 45°, and 90° (lines 5–7). Angle 0° means the propagation of laser radiation along the main axis of nanorod, angle 90° means the direction of propagation is perpendicular to the main axis, and angle 45° means intermediate position of GNR. For infinite rod, its length L is much greater than radius r_0, $L \gg r_0$. For λ= 532 nm, $K_{abs} \sim 0.3$–0.5 and $K_{sca} \sim 2$–1.2 in the range 5–100 nm for angles of irradiation 45° and 90°, and maximal values for angle 90°. Factors K_{abs} and K_{sca} for angle 0° are very small and close to 0. For wavelength 800 nm for

GNRs, values of K_{abs} are small, but values of K_{sca} for angles 45° and 90° are equal to 1.5–2.5.

For homogeneous nanorod from Eqs. 8 and 9 under $r_1=r_0$, $\rho_1=\rho_0$, $c_1=c_0$, $V_0=\pi r_0^2 L$, $S_1=2\pi r_0 L$, and $S_{10}=2\pi r_0 L$, we have for T_{max} and $\Delta T_0/I_0$:

$$T_{max} = T_\infty + \frac{2I_0 K_{abs} t_P}{\pi c_0 \rho_0 r_0} - \frac{2}{c_0 \rho_0 r_0} \int_0^{t_P} J_C dt \tag{14}$$

$$\frac{\Delta T_0}{I_0} = \frac{T_{max} - T_\infty}{I_0} = \frac{2K_{abs} t_P}{\pi c_0 \rho_0 r_0} - \frac{2}{c_0 \rho_0 r_0 I_0} \int_0^{t_P} J_C dt \tag{15}$$

For "short" pulses $t_P<\tau_{T1}$, we can get a simple equation for heating efficacy $\Delta T_0/E_0$ from Eq. 15, neglected by the loss of energy from nanorod $J_C=0$:

$$\frac{\Delta T_0}{E_0} \approx \frac{2K_{abs}}{\pi \rho_0 c_0 r_0} \tag{16}$$

It is interesting to note that for the case of "short" pulses, parameter $\Delta T_0/E_0$ depends on thermophysical, optical, and geometrical parameters of nanorod. This parameter is close to parameter (Eq. 5) for homogeneous spherical NPs, but different geometry of GNR was taken into account. GNRs with suitable aspect ratios (length divided by width) can absorb and scatter strongly in the region 700–900 nm (Huang et al. 2008), where transmissivity of tissue is maximal. Their optical resonance can be linearly tuned across the hear-infrared region by changing the effective size or the aspect ratio of the nanorods (Huang et al. 2008).

The nanorods in bioliquid (tissue) show arbitrary orientations relative to the direction of laser radiation propagation. From the other side, the optical properties of long GNRs show great dependence on angle of orientation of main axis of nanorods upon laser radiation propagation leading to decrease absorption and scattering up to ten or more times (Figs. 1 and 2). It means that some parts of GNRs with small angles of orientation will not actually take part in the processes of absorption and scattering of laser radiation. The rest of the parts of GNRs will take part in the processes of absorption and scattering of laser radiation with variable efficacy in the range 0–100%. Moreover, in some regions, collection of nanorods can have identical orientation (Huang et al. 2006), and this will be a possible situation when in some macroscopic regions, thermal effect will be realized with absorption laser energy by GNRs, but in some regions, thermal effects will be absent. In any case, these situations should be taken into account for the purposes of clinical use of GNRs.

7 Conclusion

We carried out analysis and selection of PT and PA properties of NPs using some special materials, shapes, sizes, and compositions of NPs placed in different tissues (ambiences) for laser wavelengths 532 and 800 nm on the base of the results of computer and analytical modeling. Selection and optimization of different NP types and their properties are based on investigation of the influence of different parameters of NP itself, laser pulses, and ambient tissues and fulfillment of some conditions and "confinements" on efficacies of NP applications for cancer nanotechnology.

Thermal (Eq. 1), acoustic (Eq. 2), and optical (Eq. 3) confinements should be fulfilled for the selection of the properties of NPs. Optical confinement (Eq. 3) can be realized and improved for many types of NPs by selection of optical parameters, material, sizes, and concentrations of NP. Thermal (Eq. 1) and acoustic (Eq. 2) confinements can meet three possible situations:

$t_P<\tau_A$, τ_T and $\tau_A<t_P<\tau_T$	These cases allow further NP optimization by the increase of laser heating $\Delta T_0/E_0$ (Eqs. 4 and 12) and acoustic p/E_0 (Eq. 7) efficacies and selection of thermo-optical and acoustic parameters (by increasing NP size or using ambiences with low sound speed)
$t_P>\tau_A$, τ_T	This case allows NP optimization by improvement of acoustic and thermal parameters of ambiences and efficacy of laser heating $\Delta T_0/E_0$ (Eqs. 4 and 12)

To provide penetration through small physiological pores in cell membrane and wall vessels, the radius of NP should be small enough in the range $r_0<30$–40 nm. The thermal (Eq. 1) and more strict acoustic confinement (Eq. 2) are satisfied for these sizes at the short subnanosecond and picosecond laser pulses. The use of expensive femtosecond lasers in therapeutic applications can be limited because most laser energy can be converted in ionization of NPs with subsequent plasma formation and decrease NP heating. Nanosecond lasers with $t_P\sim5$–8 ns are broadly used in laser medicine because they are simpler, less expensive than other lasers, and less harmful to healthy tissue. The condition $t_P<\tau_T$ (Eq. 1) for nanosecond lasers can be achieved for GNP by using bigger values of r_0 and smaller values of k_∞ for different ambient tissues, for example, for water $t_P\sim5\times10^{-9}$ s$<\tau_T$ for the range $r_0>70$ nm.

NPs could be placed in different ambiences (water containing tissue, blood, protein, ethanol, etc.). Optical and thermophysical properties of blood and protein are very close to water properties because these ones contain up to

60–90% of water. Spherical GNPs in the range $25<r_0<40$ nm for wavelength 532 nm can be used for laser thermal regimes for pulse durations $t_P<1\times10^{-9}$ s and acoustical regime for $t_P<3\times10^{-11}$ s in water containing tissue, blood, and protein ambiences. The use of GNPs in ethanol leads to increase of thermal and acoustic efficacies. The use of infrared wavelengths with λ=800 nm and spherical homogeneous GNPs leads to significant decrease of efficacy.

Selection of two-layered spherical NPs (core–shell: liquid–gold, silica–gold, air–gold, gold–protein, and gold–polymer) influences on efficacies of NP applications in laser medicine. Main advantage of silica–gold and water (liquid drug)–gold NPs is the possibility to tune their optical properties in visible and near-infrared regions between 500 and 1,000 nm. Under liquid–gold NP overheating because of absorption of laser energy, vapor bubble can be formed inside NP core containing liquid drug with subsequent explosion of NP and release of liquid drug on target. The feature of the practical use of air (gas)–GNPs is the possibility of the NP destruction because of increase of gas pressure with increase of NP temperature under absorption of laser energy, and pressure can be higher than the durability limit of shell. This mode could be used for fragmentation of NPs and nanophotothermolysis of cancer cells (Letfullin et al. 2006; Pustovalov et al. 2008) under much lower laser intensity I_0 in comparison with fragmentation of homogeneous GNP because of optical breakdown. Nonabsorbing layer of protein with different index of refraction in comparison with ambient bioliquid can lead to increasing of scattering efficiency factor of GNP and decreasing of heating efficacy and possibility to satisfy the optical confinement. The advantage of the use gold core–polymer shell NP could be the promotion of the fulfillment of thermal and acoustic confinements with increasing of t_P.

The gold nanorods (GNRc) placed in liquid media (water-rich tissue) show arbitrary orientations relatively on the direction of laser radiation propagation. The optical properties of long GNRs show great dependence on angle of orientation of main axis of nanorods upon direction of radiation propagation (Figs. 1 and 2) leading to decrease of absorption and scattering up to ten or more times. These situations should be taken into account for the purposes of clinical use of GNRs.

The final goal is to identify the ways to improve the increase of laser energy conversion into PT and PA phenomena by selection of the NP and ambience properties. These effects should be analyzed for different NPs using homogenous GNPs as “gold standards” for comparison.

Acknowledgements This work was supported by the National Institutes of Health/Institute of Biomedical Imaging and Bioengineering under grants EB000873 and EB0005123, and by the Arkansas Biosciences Institute for E.G. and V.P.Z.

References

Anderson RR, Parrish JA (1983) Selective photothermolysis: precise microsurgery by selective absorption of pulsed radiation. Science 220:524–527

Arakawa E, Tuminello P, Khare B, Milham M (2001) Optical properties of ovalbumin in 0, 130–2, 50 μm spectral region. Biopolymers 62:122–128

Bhandari R (1985) Scattering coefficients for a multilayered sphere: analytic expressions and algorithms. Appl Opt 24:1960–1967

Blaber MG, Arnold MD, Ford MJ (2009) Search for the ideal plasmonic nanoshells:the effects of surface scattering and alternatives to gold and silver. J Phys Chem C 113:3041–3045

Bohren CF, Huffman DR (1983) Absorption and scattering of light by small particles. Wiley, New York

Chen J, Wang D, Xi J et al (2007) Immuno gold nanocages with tailored optical properties for targeted photothermal destruction of cancer cells. Nano Lett 7:1318–1322

Eghtedari M, Oraevsky A, Copland JA, Kotov NA, Motamedi M (2007) High sensitivity of in vivo detection of gold nanorods using a laser optoacoustic imaging system. Nano Lett 7:1914–1918

Everts M, Saini V, Leddon JL et al (2006) Covalently linked Au nanoparticles to a viral vector: potential for combined photothermal and gene cancer therapy. Nano Lett 6:587–591

Grigor'ev E, Meilikhov E (eds) (1991) Physical quantities. Atomizdat, Moscow

Hirsch LR, Stafford RJ, Bankson JA et al (2003) Nanoshell-mediated near-infrared thermal therapy of tumors under magnetic resonance guidance. Proc Natl Acad Sci USA 100:13549–13554

Hirsch LR, Gobin AM, Tam F, Drezek RA, Halas NJ, West JL (2006) Metal nanoshells. Ann Biomed Eng 34:15–22

Huang X, El-Sayed IH, Qian W, El-Sayed MA (2006) Cancer cell imaging and photothermal therapy in the near-infrared region by using of gold nanorods. J Am Chem Soc 128:2115–2120

Huang X, Jain PK, El-Sayed IH, El-Sayed MA (2008) Plasmonic photothermal therapy (PPTT) using gold nanoparticles. Lasers Med Sci 23:217–228

Ivanov AP, Makarevich SA, Khairullina AY (1988) The features of propagation of radiation in tissues and bioliquids. J Appl Spectr 47:662–668

Jain PK, Lee K, El-Sayed IH, El-Sayed MA (2006) Calculated absorption and scattering properties of gold nanoparticles of different size, shape, and composition: applications in biological imaging and biomedicine. J Phys Chem B 110:7238–7248

Johnson PB, Christy RW (1972) Optical constants of the noble metals. Phys Rev B 6:4370–4378

Karabutov AA, Podymova NV, Letokhov VS (1996) Time-resolved laser optoacoustic tomography of inhomogeneous media. Appl Phys B 63:545–563

Kattawar GW, Hood DA (1976) Electromagnetic scattering from a spherical polydispersion of coated spheres. Appl Opt 15:1996–1999

Khlebtsov B, Zharov V, Melnikov A, Tuchin V, Khlebtsov N (2006) Optical amplification of photothermal therapy with gold nanoparticles and nanoclusters. Nanotechnology 17:5167–5179

Kim J-W, Galanzha E, Shashkov E, Kotagiri N, Zharov V (2007) Photothermal antimicrobial nanotherapy and nanoidiagnostics with self-assembling carbon nanotube clusters. Laser Surg Med 39:622–634

Kreith F, Black WZ (1980) Basic heat transfer. Harper and Row, New York

Letfullin RR, Joenathan C, George TF, Zharov VP (2006) Laser-induced explosion of gold nanoparticles. Nanomedicine 1:473–480

Nanospectra Biosciences, Inc (2008) Press release, July 1

Opielinski KJ (2007) Ultrasonic parameters of hen's egg. Mol Quant Acoust 28:203–217

Palik EDA (ed) (1985) Handbook of optical constants of solids. Academic, New York

Pissuwan D, Valenzuela SM, Cortie MB (2006) Therapeutic possibilities of plasmonically heated gold nanoparticles. Trends Biotechnol 24:62–67

Pitsillides CM, Joe EK, Wei X, Anderson RR, Lin CP (2003) Selective cell targeting with light-absorbing microparticles and nanoparticles. Biophys J 84:4023–4032

Pustovalov VK (2005) Theoretical study of heating of spherical nanoparticle in media by short laser pulses. Chem Phys 308:103–108

Pustovalov VK, Babenko VA (2004) Optical properties of gold nanoparticles at laser radiation wavelengths for laser applications in nanotechnology and medicine. Las Phys Lett 1:516–520

Pustovalov VK, Smetannikov AS, Zharov VP (2008) Photothermal and accompanied phenomena of selective nanophotothermolysis with gold nanoparticles and laser pulses. Las Phys Lett 5:775–792

Pustovalov V, Astafyeva L, Jean B (2009) Computer modeling of the optical properties and heating of spherical gold and silica-gold nanoparticles for laser combined imaging and photothermal treatment. Nanotechnology 20:225105

Rheims J, Köser J, Wriedt T (1997) Refractive index measurements using Abbe refractometer. Meas Sci Technol 8:601–605

Welch A, van Gemert M (eds) (1995) Optical-thermal response of laser-irradiated tissue. Plenum Press, New York

Zharov VP, Galitovsky V, Viegas M (2003) Photothermal detection of local thermal effects during selective nanophotothermolysis. Appl Phys Lett 83:4897–4899

Zharov VP, Kim J-W, Everts M, Curiel DT (2005a) Self-assembling nanoclusters in living system application for integrated photothermal nanodiagnostics and nanotherapy. Nanomedicine 1:326–345

Zharov VP, Galitovskaya EN, Jonson C, Kelly T (2005b) Sinergistic enhancement of selective nanophotothermolysis with gold nanoclusters:potential for cancer therapy. Laser Surg Med 37:219–226

Zharov VP, Mercer KE, Galitovskaya EN, Smeltzer MS (2006) Photothermal nanotherapeutics and nanodiagnostics for selective killing of bacteria targeted with gold nanoparticles. Biophys J 90:619–628

Zharov V, Galanzha E, Shashkov E, Kim J-W, Khlebtsov N, Tuchin V (2007) Photoacoustic flow cytometry: principle and application for real-time detection of circulating single nanoparticles, pathogens, and contrast dyes in vivo. J Biomed Opt 12:051503

Zuev VE (1970) Propagation of visible and infrared waves in atmosphere. Sov. Radio Press, Moscow